J. Membrane Biol. 100, 1–12 (1987)

The Journal of
Membrane Biology

Renal Basolateral Membrane Anion Transporter Characterized by a Fluorescent Disulfonic Stilbene

Pei-Yuan Chen* and A.S. Verkman

Division of Nephrology, Cardiovascular Research Institute, University of California, San Francisco, California 94143

Summary. The fluorescence enhancement of 4,4'-dibenzamido-2,2'-disulfonic stilbene (DBDS) upon binding to membranes was used to examine proximal tubule stilbene binding sites. Equilibrium binding studies of DBDS to renal brush border (BBMV) and basolateral membrane vesicles (BLMV) were performed using a fluorescence enhancement technique developed for red blood cells (A.S. Verkman, J.A. Dix and A.K. Solomon, *J. Gen. Physiol.* **81**:421–449, 1983). In the absence of transportable anions, DBDS bound reversibly to a single class of sites on BLMV isolated from rabbit (K_d = 3.8 μM) and rat (3.2 μM); 100 μM dihydro-4,4'-diisothiocyano-2,2'-disulfonic stilbene (H_2DIDS) blocked >95% of binding. H_2DIDS inhibitable DBDS binding was not detected using rat or rabbit BBMV. In rabbit BLMV, DBDS K_d doubled with 10 mM SO_4, 50 mM HCO_3 and 100 mM Cl, but was not altered by Na or pH (6–8). In stopped-flow experiments the exponential time constant for DBDS binding slowed with SO_4, HCO_3 and Cl, but was unaffected by Na. These results are consistent with competitive binding of DBDS and anions at an anion transport site. To relate DBDS binding data to anion transport inhibition we used $^{35}SO_4$ uptake to characterize several modes of rabbit BLM anion transport: H/SO_4 and Na/SO_4 cotransport, and Cl/SO_4 countertransport. Each transport process was electroneutral and was inhibited by H_2DIDS, furosemide, probenecid, chlorothiazide and DBDS. The apparent K_i's for DBDS (3–20 μM) were similar to K_d for DBDS binding. These studies define a class of anion transport sites on the proximal tubule basolateral membrane measureable optically by a fluorescent stilbene.

Key Words proximal tubule · basolateral membrane · anion transport · disulfonic stilbene · fluorescence

Abbreviations

BBMV: brush border membrane vesicle
Bicin: N,N'-bis(2-hydroxyethyl)glycine
Bis-Tris: bis(2-hydroxyethyl)iminotris(hydroxymethyl)methane
BLMV: basolateral membrane vesicle
CCCP: carbonylcyanide-*m*-chlorophenylhydrazone
DBDS: 4,4'-dibenzamido-2,2'-disulfonic stilbene
DIDS: 4,4'-diisothiocyano-2,2'-disulfonic stilbene
H_2DIDS: dihydro-4,4'-diisothiocyano-2,2'-disulfonic stilbene
HEPES: 4-(2-hydroxyethyl)-1-piperazineethanesulfonic acid
NMG: N-methylglucamine
SITS: 4-acetamido-4'-isothiocyano-2,2'-disulfonic stilbene
Tris: tris(hydroxymethyl)aminomethane

* *Present address:* Department of Internal Medicine, Taipei Medical College, 252 Wu-Hsing St., Taipei, Taiwan.

Introduction

Anion transport in the mammalian proximal tubule has an important role in the transcellular resorption of anions including Cl, SO_4 and HCO_3 filtered by the glomerulus. A number of anion transport systems have been described recently in brush border and basolateral membrane vesicles isolated from the renal cortex of rat, dog and rabbit as reviewed in the Discussion section [2, 3, 11, 12, 14, 15, 20, 27]. In general, epithelial cell basolateral membranes often have anion/anion countertransport with broad specificity and Na-coupled anion transport; brush border membranes often have Cl/anion exchange and Na-driven anion cotransport. These transport systems have variable sensitivities to disulfonic stilbenes. It is not known which protein or proteins mediate proximal tubule anion transport, whether these proteins constitute a major portion of total membrane protein, and what the mechanism for stilbene inhibition of anion transport is.

We have used the stilbene derivitive 4,4'-dibenzamido-2,2'-disulfonic stilbene (DBDS) to characterize anion transport systems in brush border and basolateral membrane vesicles isolated from rabbit and rat renal cortex. The fluorescence of DBDS increases by 1–2 orders of magnitude when bound to a nonpolar site (membrane protein), providing an optical marker for anion transport proteins. We used DBDS fluorescence previously to characterize the nature of the stilbene binding site on red cell band 3 [7, 28], and to examine the mechanisms by which chloride, phloretin, *p*-chloromercuribenzenesulfonate (*p*CMBS) and general anesthetics alter band 3 function and conformational state [6, 9, 10, 21].

Based on equilibrium and kinetic studies of DBDS binding to renal vesicles, we identified a

class of H_2DIDS inhibitable DBDS binding sites on renal basolateral membranes which were not present on brush border membranes. DBDS binding affinities and binding rates were decreased by SO_4, HCO_3 and Cl, and not by Na or pH. By assuming comparable quantum efficiencies and molecular sizes for the band 3-DBDS complex and for the basolateral anion transporter-DBDS complex, it was estimated that basolateral anion transporter(s) account for ~20% of total basolateral membrane protein. To relate DBDS binding characteristics to DBDS inhibition of basolateral anion transport, we measured the potency (K_I) for DBDS inhibition of several modes of basolateral anion transport which have not been studied previously in rabbit basolateral membrane vesicles: anion, pH and Na gradient driven SO_4 influx. We conclude that DBDS binds to a basolateral membrane anion transporter which constitutes a significant fraction of total membrane protein, where it inhibits an electroneutral anion transport process with high affinity (<20 μM).

Materials and Methods

Materials

$H_2{}^{35}SO_4$ (10 mCi/mg) was obtained from New England Nuclear (Bedford, MA). H_2DIDS and SITS were obtained from Molecular Probes (Junction City, OR), and DBDS was synthesized by the method of Kotaki et al. [18]. Stilbenes were stored as 1 mM aqueous solutions in the dark at 4°C; DBDS does not undergo significant *cis-trans* isomerization under these conditions [28]. Probenecid, furosemide and chlorothiazide were prepared as stock solutions in ethanol. All other chemicals were obtained from Sigma Chemical Co. (St. Louis, MO).

Membrane Preparations

Unsealed red cell ghost membranes were prepared from recently outdated blood as described previously [8]. BBMV and BLMV were isolated from renal cortex of 1–2 kg New Zealand white rabbits and 300–350 g male Wistar rats. Animals were sacrificed by decapitation, and the renal artery was perfused with iced buffered saline until complete blanching occurred. Renal cortex was dissected and homogenized using a Sorvall-Omni mixer for 4 min at 4°C in 250 mM sucrose, 10 mM HEPES/Tris, 5 mM EGTA, pH 7.0. BBMV were isolated by a Mg-aggregration and differential centrifugation procedure [4]. BLMV were isolated by centrifugation for 16 hr at 100,000 × g, 4°C using a 35–48% linear sucrose density gradient [17, 29]. Gradient fractions were collected and assayed for maltase (apical membrane marker) and ouabain-inhibitable Na/K ATPase (basolateral membrane marker) activities. The fractions with highest Na/K ATPase and lowest maltase activities were pooled, typically at densities of 1.14 to 1.15 g/ml.

Marker enzyme activities were measured and found similar to those reported previously [17, 29]. BBMV were enriched in maltase specific activity >15-fold over crude homogenate and in Na/K ATPase activity <0.3-fold. BLMV ouabain-inhibitable Na/K ATPase activity was enriched >15 fold and maltase activity was enriched 0.2–0.3-fold over crude homogenate. Succinate dehydrogenase activity was reduced >95% in all preparations. As reported by Akiba et al. [2], measurements of latency of Na/K ATPase activity in the presence and absence of deoxycholate showed that BLMV were >55% sealed; of the sealed vesicles, >95% were right-side out. BBMV and BLMV were pelleted, resuspended in 50 volumes of the desired buffer at 4°C for at least 24 hr and repelleted (40,000 × g, 40 min) before experimentation.

Equilibrium DBDS Binding Experiments

Equilibrium binding of DBDS to membranes (ghosts, BBMV and BLMV) was determined by a fluorescence enhancement technique as detailed previously [7, 28]. The fluorescence of membrane suspensions (~0.2 mg protein/ml) titrated with increasing [DBDS] (typically 0–20 μM) was measured (excitation 360 nm, emission 420 nm, 8 nm monochromator bandpass) in a SLM 8225 fluorimeter (SLM Instruments, Urbana, IL). At least 30 sec were allowed to elapse between the time of each DBDS addition and measurement of fluorescence, at which time the fluorescence intensity was stable. The measured fluorescence (F_{meas}) was assumed to be proportional to bound DBDS after corrections were made for membrane scattering (F_{scat}), fluorescence of aqueous DBDS (F_{DBDS}) and inner filter effects [28].

$$F_{meas} = Q(F_{corr} + F_{scat}) + F_{DBDS} \quad (1)$$

where F_{corr} is the corrected fluorescence. Q is an inner filter correction determined by fitting F_{DBDS} *vs.* [DBDS] in the absence of membranes to a quadratic function (A[DBDS]^2 + B[DBDS] + C); Q is equal to $B/(B + A[DBDS])$ and typically ranges from 0.95 (<1 μM DBDS) to 0.6 (20 μM DBDS) [28].

F_{corr} *vs.* [DBDS] data were fitted to a saturable, single-site binding model using a 3-parameter nonlinear Newton fitting procedure,

$$F_{corr} = F_o[DBDS]/(K_d + [DBDS]) + F_{ns}[DBDS] \quad (2)$$

where F_o is the maximum fluorescence of DBDS bound to specific binding sites (fluorescence units, *FU*), K_d is a single-site dissociation constant (μM) and F_{ns} quantitates nonspecific DBDS binding to membrane proteins and phospholipids (FU/μM). As given in the Results section, nonspecific binding accounted for <5% of fluorescence at 3 μM DBDS and ~30% of fluorescence at 15 μM DBDS.

DBDS Binding Kinetics

Kinetics of DBDS binding to membranes was measured using a Dionex-130 stopped-flow apparatus (Sunnyvale, CA) which has a dead time of <2 msec and a maximum rate of data acquisition of 512 points in 40 msec. 0.1 ml of solution containing membranes (0.5–2 mg protein/ml) was mixed with an equal volume of solution containing DBDS (0–32 μM). The time course of increasing fluorescence ($F(t)$) was recorded on a MINC/23 computer (Digital Equipment Corp., Maynard, MA) for analysis. Fluorescence was excited using a 150-W Hg-Xenon arc lamp and a Zeiss MM12 double monochromator set at 360 nm with 20 nm bandpass; emission fluorescence was filtered by a Corion 400 nm cut-on filter. $F(t)$ data were fitted to single exponential functions.

$^{35}SO_4$ Uptake Studies

$^{35}SO_4$ uptake was measured at 23°C by the rapid filtration method. Uptake was initiated by mixing 10 μl of BLMV (~10 mg protein/ml) with 190 μl of solution containing $^{35}SO_4$. Inhibitors, when present, were present in both solutions. The composition of intravesicular and solutions buffers, and the concentrations of valinomycin and CCCP are given in the figure and table legends. Transport was stopped after a specified time interval by addition of 2 ml of stop solution (150 mM NaCl, 10 mM HEPES/Tris, 10 mM K_2SO_4, 50 μM SITS, pH 7, 4°C), and filtered immediately on 0.65 μm HAWP Millipore filters (Bedford, MA), prewetted with 100 mM K_2SO_4, under vacuum pump suction. The filters were washed three additional times with 2 ml of stop solution, dissolved in Scinti Verse Bio-HP scintillation fluid (Fisher Scientific, Fairland, NJ) and counted in a 6847 Nuclear Chicago Counter (TM Analytic, Elk Grove Village, IL). Filtration and washing were completed in under 10 sec. Nonspecific binding of $^{35}SO_4$ was subtracted in every experiment. Unless stated, each experiment was performed in quadruplicate using at least three different membrane preparations.

SPQ Fluorescence Experiments

Cl influx into BLMV was monitored using the entrapped Cl-sensitive fluorescent indicator 6-methoxy-N-[3-sulfopropyl] quinolinium (SPQ) [16]. BLMV were loaded with 10 mM SPQ by incubation for 18 hr at 4°C. Extravesicular SPQ was removed by three washes in >25 volumes of buffer not containing SPQ. Cl influx experiments were initiated by adding BLMV in buffer containing 250 mM sucrose, 50 mM K gluconate, 100 NMG gluconate, 10 mM HEPES/Tris, pH 7.0 to 2 ml of isotonic, isosmotic buffer containing 50 mM Cl. In some experiments, K gluconate was replaced by 10 mM K_2SO_4; ionic strength was balanced by addition of NMG gluconate. Fluorescence was monitored at excitation and emission wavelengths of 350 and 450 nm, respectively. Cl flux in units of nmol/sec/mg protein was calculated from the fluorescence data as described previously [5, 16].

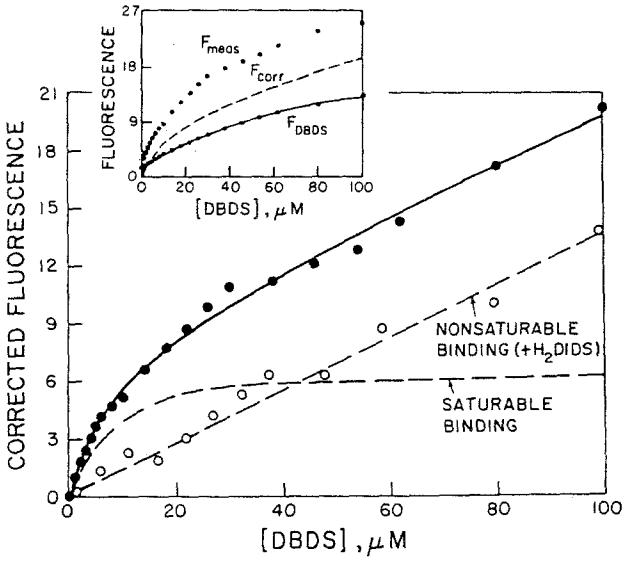

Fig. 1. Fluorescence titration of DBDS binding to BLMV. Increasing concentrations of DBDS were added to rabbit BLMV (0.4 mg/ml) in a 2 × 10 mm pathlength quartz cuvette as described in Materials and Methods. Experiments were performed in the absence (filled circles) and presence (open circles) of 500 μM H_2DIDS to block the saturable binding component. Buffer consisted of 250 mM sucrose, 50 mM K-gluconate, 100 NMG gluconate, 10 mM HEPES/Tris, pH 7.0, 23°C. Corrected fluorescence data were fitted to the single site binding model in Eq. (2) with F_o = 6.3 fluorescence units, K_d = 5 μM and F_{ns} = 0.13 fluorescence units/μM. Saturable and nonsaturable components of binding calculated from the fitting procedure are shown as dashed curves. Inset: Uncorrected fluorescence measured in the presence (F_{meas}) and absence (F_{DBDS}) of BLMV, and the fitted curve for corrected fluorescence (F_{corr}) are plotted against [DBDS]. The F_{DBDS} *vs.* [DBDS] data were fitted to the quadratic $A[DBDS]^2 + B[DBDS] + C$ with B/A = 239 μM

Results

Equilibrium DBDS Binding

Upon addition of increasing [DBDS] to membrane vesicles containing stilbene binding sites, there is an increase in measured fluorescence intensity resulting from several processes: (i) fluorescence of aqueous DBDS, (ii) fluorescence of DBDS bound to saturable sites (protein), and (iii) fluorescence of DBDS bound to nonsaturable sites (predominantly lipid). In addition, some excitation light scattered from the vesicles is measured, and an inner filter correction is required to correct measured fluorescence for absorption of excitation and emission light by DBDS (*see* Materials and Methods). These corrections become increasingly important for [DBDS] > 10 μM and when the fluorescence signal arising from DBDS bound to saturable binding sites is small.

To delineate the presence of both saturable and nonsaturable DBDS binding sites on rabbit BLMV, a fluorescence titration was performed using a cuvette with reduced excitation pathlength (2 mm) to minimize inner filter correction at high [DBDS] (Fig. 1). The fluorescence, corrected for aqueous DBDS, membrane scattering and inner filter effects (F_{corr}; Eq. (1)), is plotted on the y axis. The figure inset gives the raw data for F_{meas} and F_{DBDS} as a function of [DBDS]. Both saturable and nonsaturable components of DBDS binding are present. The saturable binding component was absent in a similar experiment performed in the presence of 500 μM H_2DIDS, a high affinity, nonfluorescent stilbene. The presence of two types of binding sites is supported by kinetic experiments (below) in which it is shown that nonsaturable binding occurs in <2 msec, whereas saturable binding occurs in >100 msec and is inhibitable by H_2DIDS and several anions.

The effect of H_2DIDS on equilibrium binding of

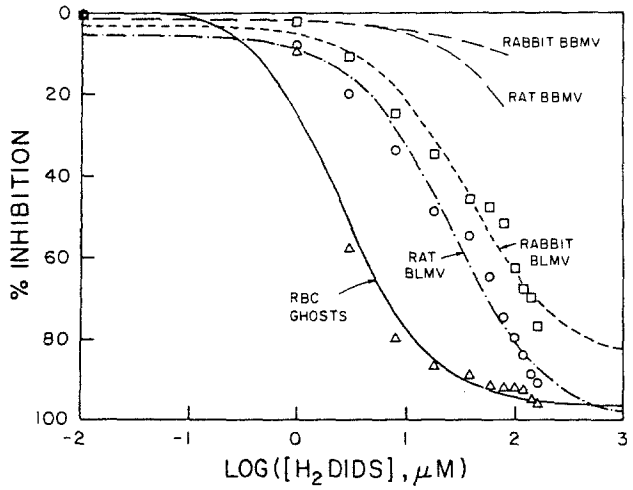

Fig. 2. Inhibition of DBDS binding by H_2DIDS. Increasing concentrations of H_2DIDS were added to a cuvette containing various membrane preparations (0.1–0.2 mg/ml) and 4 μM DBDS using the buffer system given in the legend to Fig. 1. The % inhibition was determined from the ratio of corrected fluorescence values measured in the absence and presence of H_2DIDS. For clarity, the individual data points are not shown for rat and rabbit BBMV. Data were fitted to a saturable, single-site binding model with K_d = 2.4 μM (RBC ghosts), 25 μM (rat BLMV), 35 μM (rabbit BLMV), >100 μM (rat BBMV) and >100 μM (rabbit BBMV)

DBDS to red cell ghosts, and to BBMV and BLMV isolated from rat and rabbit is shown in Fig. 2. The experiment was performed using 4 μM DBDS, a concentration near the K_d at which relatively little nonsaturable DBDS binding occurs. While there was strong inhibition of DBDS binding to ghosts and to BLMV by H_2DIDS, there was little H_2DIDS-inhibitable DBDS binding to BBMV. The quantity of H_2DIDS-inhibitable DBDS binding to BLMV, expressed as fluorescence per mg of vesicle protein (Table 1), is ~38% of that measured for binding to band 3 in red cell membranes. It is known that band 3 constitutes ~50% of red cell membrane protein. If the basolateral membrane anion transporter has similar molecular weight to band 3 (95 kDa), and if the quantum yields and molar absorptivities of DBDS bound to sites on band 3 and the BLMV membrane are similar, then the basolateral membrane anion transporter(s) constitutes ~20% of total basolateral membrane protein. The small quantity of DBDS binding to BBMV may represent contamination by BLMV or DBDS binding to a BBMV anion transporter present in relatively small numbers or having low stilbene binding affinity (*see* Discussion).

In red cell ghost membranes, DBDS binding affinity is decreased by transportable anions such as Cl [6] and by a number of inhibitor compounds which bind to band 3 including phloretin and

Table 1. Equilibrium DBDS binding to red cell ghosts and to renal membranes

	K_d (μM)	F_n (FU)	[protein] (mg/ml)	Relative binding (%)
RBC ghosts	0.93	9.9	6.5	100
Rab BLMV	3.2	4.7	9.9	31
Rabbit BLMV	3.8	5.9	10.2	38
Rat BBMV	>10	<0.2	13.6	<2
Rabbit BBMV	>10	<0.2	13.1	<2

DBDS binding was measured as described in Materials and Methods in the absence of transportable anions. F_n represents the H_2DIDS inhibitable fraction of DBDS binding; F_n and K_d were fitted using Eq. (2) for RBC ghosts and BLMV. Protein concentration for each sample was measured by the Lowry method. Relative binding represents F_n/[protein] in each membrane relative to that in RBC ghosts.

pCMBS [9, 21]. We examined the effect of Cl, SO_4, HCO_3, Na and pH on the K_d for DBDS binding to rabbit BLMV (Table 2). There was no effect of Na or pH in the range 6–8 (*data not given*) on K_d, whereas the anions decreased DBDS binding affinity with relative potencies $SO_4 > HCO_3 > Cl$. These results are consistent with a competitive interaction between DBDS and anions at a basolateral membrane anion transport site. To determine semi-quantitatively whether other anions interacted with the DBDS binding site, the corrected fluorescence of bound DBDS (F_{corr}) was measured using conditions given in the legend to Fig. 2 (4 μM DBDS, 0.1 mg/ml BLMV) for 10 mM anion concentrations. Relative F_{corr} values were: 1.0 (gluconate), 0.45 (formate), 0.42 (acetate), 0.35 (lactate) and 0.30 (sulfate). Therefore a series of anions appear to alter equilibrium DBDS binding. With increasing temperature in the absence of transportable anions, K_d increased (2.9 ± 0.9 μM, 14°C; 3.8 ± 0.6 μM, 23°C; 6.1 ± 1 μM, 46°C) in a manner similar to results for DBDS binding to red cell ghosts [28].

DBDS Binding Kinetics

Stopped-flow kinetic measurements were performed to define further the mechanism of interaction between DBDS and the anion transporter. Upon rapid mixing of DBDS with BLMV in the absence of transportable anions, there is a biexponential time course of increasing fluorescence with time constants of 150 msec and 6.3 sec which is blocked completely by preincubation of BLMV with 0.5 mM H_2DIDS (Fig. 3). Similar time courses were observed with time constants of 200 msec and 5.5 sec using rat BLMV. No time course of increasing fluorescence was observed for mixture of DBDS

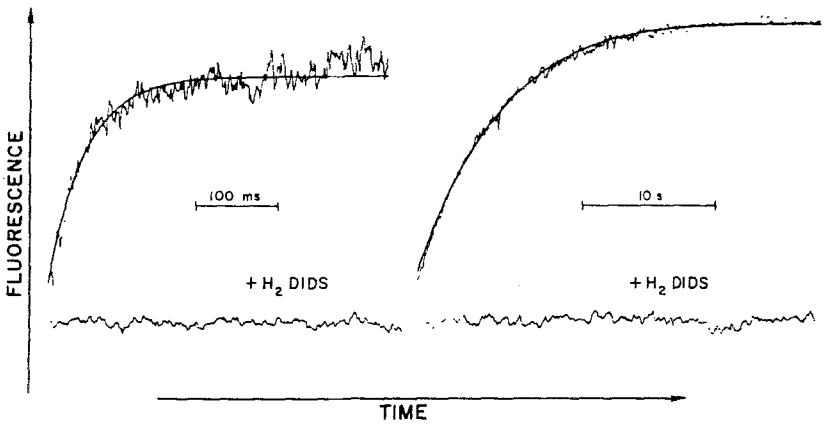

Fig. 3. Time course of DBDS binding to rabbit BLMV. BLMV (1 mg protein/ml) were mixed with an equal volume of buffer containing 16 μM DBDS in 250 mM sucrose, 50 mM K gluconate, 100 NMG gluconate, 10 mM HEPES/Tris, pH 7.0, 23°C in a stopped-flow apparatus. The time course increasing fluorescence intensity corresponds to DBDS binding. Data are shown using two different time scales with fitted single exponential time constants of 150 msec and 6.3 sec. Addition of 0.5 mM H_2DIDS to the BLMV solution abolishes the time course of increasing fluorescence

Table 2. Equilibrium DBDS binding to rabbit BLMV

Ion	Concentration (mM)	K_d (μM)	τ_{fast} (msec)	τ_{slow} (sec)
Control		3.8 ± 0.6	152 ± 4	6.2 ± 0.4
SO_4	10	7.7 ± 1		
	25		320 ± 60	6.1 ± 0.2
HCO_3	25		780 ± 100	5.2 ± 0.5
	50	7.0 ± 0.8		
Cl	25		271 ± 30	5.4 ± 0.4
	100	6.3 ± 1		
Na	100	3.7 ± 0.4	168 ± 14	6.3 ± 0.8

DBDS binding was measured in rabbit BLMV in the absence of transportable anions (NMG gluconate, control) and with NMG gluconate replaced by specified concentrations of possible transportable ions. K_d, τ_{fast} and τ_{slow} were determined as described in the legends to Figs. 3 and 4.

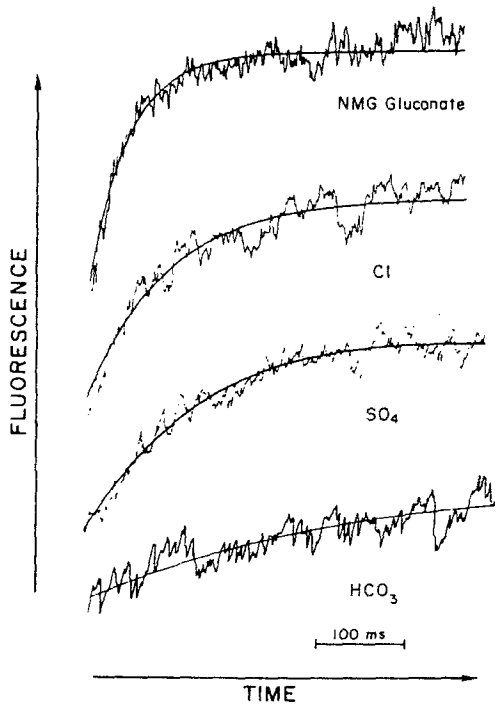

Fig. 4. Effects of anions on kinetics of DBDS binding to BLMV. Stopped-flow experiments were performed as in Fig. 3 with replacement of 100 mM NMG gluconate with 75 mM NMG gluconate + 25 mM NMG-anion. Fitted single exponential time constants are summarized in Table 2.

with BBMV from rat or rabbit, with phosphatidylcholine vesicles (200 μM phospholipid) and with vesicles prepared from lipid extracted from red blood cells [28]. We conclude that the time course of increasing fluorescence is associated with binding of DBDS to saturable sites; binding of DBDS to nonsaturable sites (primarily phospholipid) occurs within the dead time of the stopped-flow instrument (2 msec).

The effect of anions and Na on DBDS binding kinetics is summarized in Table 2; representative time course data are given in Fig. 4. There is no effect of Na on the time course, whereas SO_4, HCO_3 and Cl slow the time constant for the first exponential. The slow time constant is not altered by any of the ions or by a change in [DBDS] (2–16 μM; *data not shown*). Based on DBDS transport data using inside-out red cell vesicles [28], the slower exponential may represent transmembrane DBDS passage and binding to H_2DIDS-inhibitable sites on the inside vesicle surface. Other interpretations cannot be excluded from the data presented, including: (i) DBDS binding to an independent class of external binding sites which are H_2DIDS but not anion inhibitable, and (ii) sequential DBDS binding in which a slow conformational change in a single DBDS-binding protein (following the faster conformational change) causes a further enhancement in DBDS fluorescence.

The slowing of the measured fast time constant for DBDS binding to BLMV by Cl, SO_4 and HCO_3 is opposite to that observed in red cell ghost membranes [6], where it was concluded that DBDS and transportable anions occupy distinct binding sites

which interact in a noncompetitive manner. The decrease in DBDS binding affinity and binding rate in BLMV are compatible with competitive interaction between stilbenes and transportable anions at a single binding site.

In red cell ghost membranes it was possible to define the precise mechanism by which Cl modified the band 3-DBDS binding interaction from the measured dependences of the binding time course on [DBDS] and [Cl] [6, 28]. It was concluded that the measured binding time course is the rate-limiting band 3-DBDS conformational change which followed a rapid bimolecular association reaction between band 3 and DBDS. Only a limited study of the dependence of the fast exponential time constant on [DBDS] was possible using rabbit BLMV because of the small signal amplitude and the rapid time course compared with that measured in red cell ghosts. For mixture of BLMV (1 mg protein/ml) with DBDS to give final DBDS concentrations of 2, 4, 8 and 16 μM, fitted exponential time constants were 151 ± 20 msec, 171 ± 13 msec, 179 ± 6 msec and 195 ± 15 msec, respectively (SD, $n = 3$ for each measurement). The lack of significant dependence of the time constant on [DBDS] over an eightfold concentration range suggests that the measured binding time course in BLMV represents a rate-limiting unimolecular reaction (conformational change). Because the fluorescence signal was very poor below 2 μM DBDS, it was not possible to study the association reaction which must precede the conformational change. Interestingly, the rate of the BLMV-DBDS conformational change (5–6 sec^{-1}) is very similar to that measured in red cell ghost membranes (4 sec^{-1}; ref 28), whereas the BLMV-DBDS binding affinity (3 μM) is much lower than that measured in ghosts (<0.1 μM).

Anion Transport Measurements

Measurements of rabbit BLMV anion transport were performed to examine the physiological function of the DBDS-binding protein identified from fluorescence measurements. In BLMV isolated from dog, rat and marine teleost, several modes of SO_4 transport have been identified in which SO_4 movement is driven by *cis*-H gradients, *trans*-anion gradients and *cis*-Na gradients [3, 15, 20, 24, 25]. In addition, neutral Cl/HCO_3 and electrogenic Na-driven 3HCO_3 transport have been identified in BLMV isolated from rabbit [2, 11]. The first set of experiments were designed to determine the modes and properties of anion transport present in rabbit BLMV which have not been studied previously. The dose response for DBDS inhibition of anion transport will then be determined.

Table 3. Influence of K diffusion potentials on SO_4 uptake

	$[K]_{out}/[K]_{in}$		
	100/5	100/100	5/100
pH driven	165 ± 6	160 ± 13	185 ± 20
Na driven	78 ± 1	72 ± 5	78 ± 5
Cl driven	44 ± 2	42 ± 2	41 ± 3

Experiments were performed as described in the legend to Fig. 5 with specified K gradients obtained by replacing K with NMG. Data represent mean ± SD $^{35}SO_4$ uptake in pmol/mg protein for one set of experiments (typical of two) performed in quadruplicate with background subtrated. Incubation times were 4 sec (pH driven), 10 sec (Cl driven) and 10 sec (Na driven).

The time course of $^{35}SO_4$ influx into rabbit BLMV stimulated by inwardly directed H and Na gradients, and by outwardly directed Cl gradients is shown in Fig. 5. To prevent coupling of SO_4 transport to other ion gradients by induced diffusion potentials, BLMV were voltage clamped with K and valinomycin. For experiments involving Na and Cl-gradient driven SO_4 transport, BLMV were also pH clamped using CCCP to prevent coupling of SO_4 transport to pH gradients which might be induced by the ion gradients. Any enhancement of SO_4 transport by ion gradients thus indicates the presence of a protein-mediated countertransport process. The data in Fig. 5 show an overshoot in SO_4 uptake, indicating that all three modes of SO_4 transport are present in rabbit BLMV. The electrical properties of each mode of transport were examined from the effective of K diffusion potentials on SO_4 influx measured at a single time point, where SO_4 uptake is approximately linear with time (Table 3). Because influx rates were unchanged by induced diffusion potentials, it is concluded that each mode of SO_4 transport is electroneutral under the conditions of the experiment.

The anion specificities of the BLMV SO_4 transporter are shown in Fig. 6, top. Under voltage and pH-clamped conditions, SO_4 influx is *trans*-stimulated by a series of anions, notably including Cl and HCO_3. The dose-response relation for trans-stimulation of tracer $^{35}SO_4$ influx by internal Cl and HCO_3 is given in Fig. 6, bottom. Fitted K_d's for Cl and HCO_3 were 16 and 20 mM. Thus, the basolateral membrane SO_4 (anion) transport is saturable and operates in an exchange mode with broad anion specificity, similar to the properties of red cell band 3. The relativity high K_d's of the transporter for Cl and HCO_3 suggest that these ions can regulate the activity of the SO_4 transporter under physiological conditions.

The inhibitory properties of the BLMV SO_4

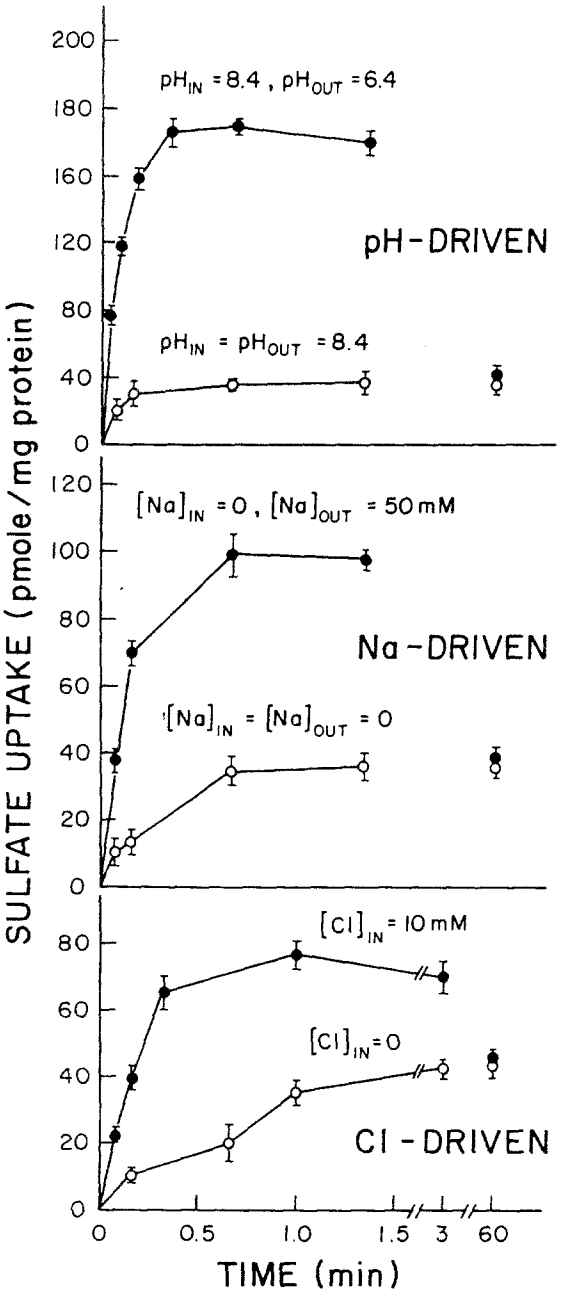

Fig. 5. Time course of $^{35}SO_4$ uptake driven by H, Na and Cl gradients in rabbit BLMV. *Top:* H-driven SO_4 transport. Ten μl BLMV (10 mg protein/ml, 50 mg valinomycin/mg protein) in 250 mM sucrose, 100 mM K gluconate, 50 mM Bicin/Tris, pH 8.4, was diluted into 190 μl buffer containing 250 mM sucrose, 100 mM K gluconate, 50 mM bis-Tris, and tracer $H_2{}^{35}SO_4$, pH 6.4, 23°C ($pH_{in} < pH_{out}$) or 190 μl of the Bicin/Tris buffer at pH 8.4 containing $^{35}SO_4$ ($pH_{in} = pH_{out}$). *Middle:* Cl-driven SO_4 transport. Ten μl BLMV (10 mg protein/ml, 50 mg valinomycin/mg protein, 5 μM CCCP) in 250 mM sucrose, 50 mM NMG gluconate, 90 mM K gluconate, 10 HEPES/Tris, $^{35}SO_4$, pH 7.0 containing 10 mM KCl or K gluconate were diluted into 190 μl of the same buffer without Cl. *Bottom:* Na-driven SO_4 transport. BLMV containing valinomycin/CCCP in Na-free buffer (same as 0 Cl buffer used in Cl experiments) or Na-containing buffer (250 mM sucrose, 100 mM K gluconate, 50 mM Na gluconate, 10 HEPES/Tris, pH 7.4) were diluted into Na-free or Na-containing buffer with $^{35}SO_4$. Uptake measurements expressed as pmol SO_4/mg vesicle protein, determined using tracer $^{35}SO_4$, are the mean ± SD of four measurements

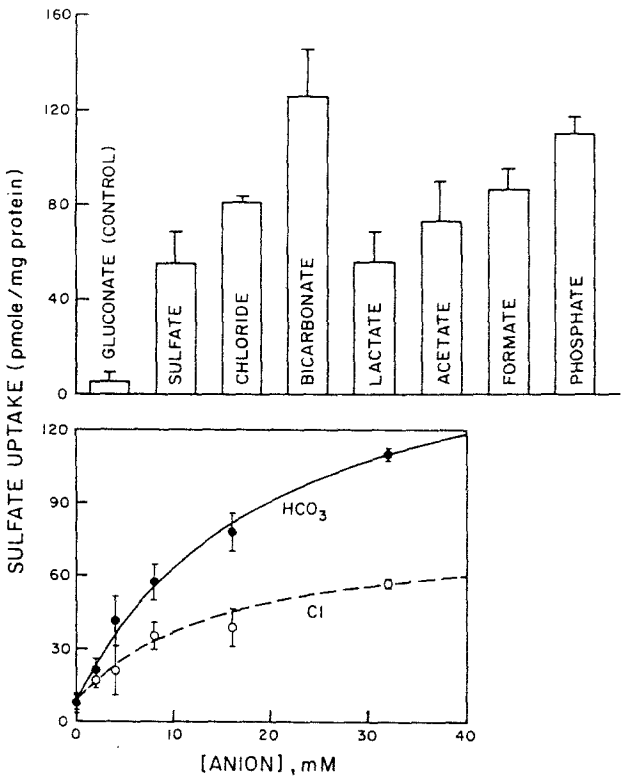

Fig. 6. Stimulation of SO_4 influx by *trans*-anion gradients. *Top:* 10 μl of rabbit BLMV (10 mg protein/ml) containing valinomycin/CCCP in 250 mM sucrose, 80–90 mM K gluconate, 50 mM NMG gluconate, 10 mM HEPES/Tris and 10 mM K-anion, pH 7.0, were diluted into 190 μl of identical buffer containing gluconate and $^{35}SO_4$. Each point represents the mean ± SD of quadruplicate measurements of 10 sec uptake. Uptake at 0 sec, representing nonspecific binding to filters and to BLMV, was subtracted in each measurement. In control experiments, there was no effect of anions at 0.5 mM concentration in the external solution on $^{35}SO_4$ influx measured in the absence of *trans*-anion gradients. Therefore preloaded anions carried over into the external solution in *trans*-stimulation experiments do not affect measured SO_4 influx. *Bottom:* HCO_3 and Cl concentration dependences of SO_4 uptake. Experiments were performed as above with K-gluconate replaced by KCl or $KHCO_3$ at various concentrations. For HCO_3 experiments, 50 mM HEPES/Tris buffer was used to clamp buffer pH. Each point is the mean ± SD of quadruplicate measurements. Data were fitted to a saturable, single-site binding model with K_d = 16 ± 5 mM (Cl) and 20 ± 3 mM (HCO_3) and V_{max} 73 pmol/mg (Cl) and 165 pmol/mg (HCO_3)

transporter are summarized in Fig. 7. There is inhibition of H, Cl and Na-gradient driven SO_4 influx by 0.5 mM stilbene (H_2DIDS and SITS), and 1 mM furosemide, probenecid and chlorothiazide; there was no effect of 1 mM amiloride and acetazolamide. This pattern is similar to that observed for anion transporters such as red cell band 3; however, the inhibition of SO_4 transport by chlorothiazide was unexpected because this compound is not known to alter proximal tubule function.

The anion specificity for *cis*-inhibition of H and Na gradient-driven SO_4 influx is shown in Fig. 8. At

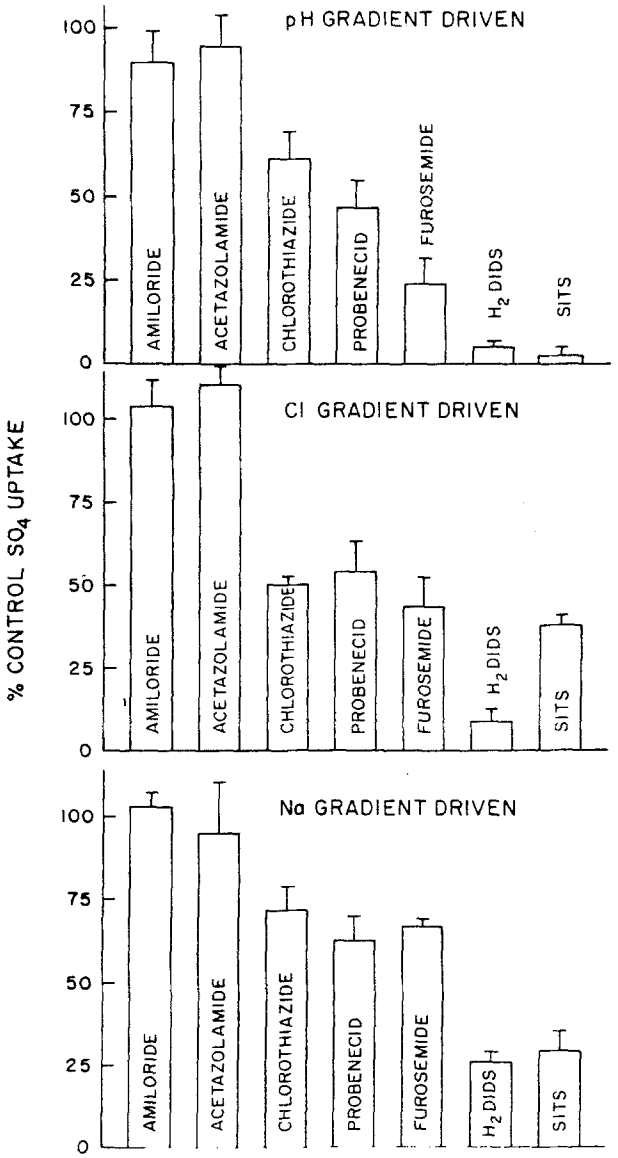

Fig. 7. Inhibition of SO_4 uptake. H and Cl and Na-gradient driven SO_4 influx were measured under conditions given in the legend to Fig. 5. Inhibitors (all 1 mM except H_2DIDS and SITS, 0.5 mM) were incubated with BLMV for 30 min prior to experiments and were also present in the dilution buffer. SO_4 uptake is expressed as the percentage inhibition of control uptake in the absence of inhibitors (mean ± SD) for quadruplicate determinations

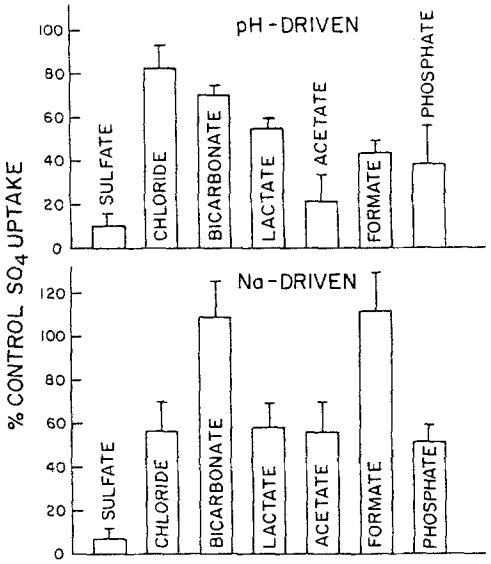

Fig. 8. *Cis* inhibition of SO_4 transport. H and Na-gradient driven SO_4 uptake were measured under conditions given in the legend to Fig. 5 in the presence of a 10-mM anion concentration in the external buffer, replacing gluconate. Uptake is expressed as the percentage (mean ± SD) of control uptake determined with 100 mM NMG gluconate in the external solution

Table 4. *Cis*-inhibition of $^{35}SO_4$ uptake by SO_4

$[SO_4]$ (μM)	pH driven (% control)	Na driven (% control)
0.1 (control)	100	100
5	99 ± 9	100 ± 4
10	87 ± 8	101 ± 4
20	73 ± 4	
40	17 ± 2	88 ± 7
80	10 ± 2	71 ± 8
160	10 ± 1	62 ± 10
1,000	3 ± 2	62 ± 9
10,000	10 ± 6	7 ± 5

H and Na-gradient driven $^{35}SO_4$ influx was measured as described in the legend to Fig. 5 with variable external SO_4. Transport rates are expressed as % of control (mean ± SD) measured at tracer SO_4 concentration for one set of experiments (typical of two) performed in quadruplicate. Data were fitted to a single site, saturable inhibition model with K_I = 30 μM (pH driven) and 1500 μM (Na driven).

10 mM anion concentrations, there was ~90% *cis*-inhibition by SO_4 with lesser or no inhibition by the other anions. Interestingly, the pattern of anion potencies for *cis*-inhibition of H-driven SO_4 uptake were quite different from that of Na-driven SO_4 uptake, suggesting that these transporters may be distinct.

To examine further the differences in transport characteristics of these systems, the dose-responses for *cis*-SO_4 and DBDS inhibition were measured (Table 4 and Fig. 9). For H gradient-stimulated SO_4 uptake there is a remarkably low K_I of ~30 μM. In contrast, K_I for SO_4 inhibition of Na gradient stimulated SO_4 transport is >1000 μM. These results support the possibility that Na/SO_4 and H/SO_4 (OH/SO_4) transport occur via different routes.

The dose-response relations for DBDS inhibition of $^{35}SO_4$ influx driven by inwardly directed H and Na gradients are given in Fig. 9. For Na/SO_4

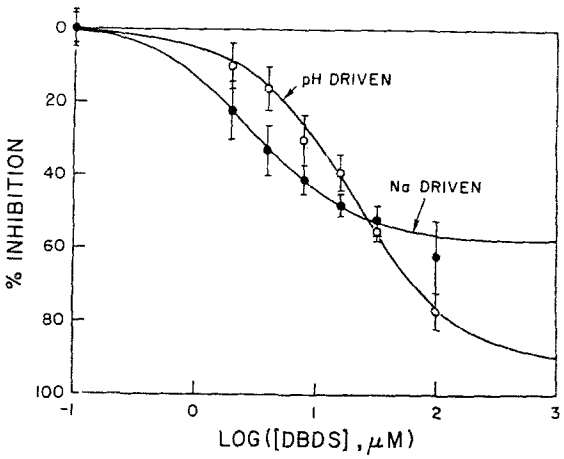

Fig. 9. DBDS inhibition of SO_4 influx. pH and Na gradient driven $^{35}SO_4$ influx was measured in quadruplicate using the methods given in the legend to Fig. 5 using a 4-sec time point for pH-driven transport and a 10 sec time point for Na driven transport. Data were fitted to a saturable, single-size inhibition model with K_I = 20 μM (pH driven) and 3.2 μM (Na driven)

transport, the K_I for DBDS inhibition (~3 μM) is similar to the K_d for DBDS binding measured in the absence of transportable anions. The K_d for DBDS inhibition of H-driven SO_4 influx is larger (20 μM), consistent with the possibility that the transport proteins for Na/SO_4 and H/SO_4 cotransport are different. It is unlikely that the differences in K_d are due to a competitive interaction between H/OH and DBDS for binding to the anion transport site because there was no measured effect of pH on the DBDS binding affinity.

To demonstrate that the measured Na/SO_4 cotransport is a property of the basolateral membrane and not due to brush border contamination, $^{35}SO_4$ uptake measurements were performed on BBMV. For experiments performed on BBMV under conditions identical to those used in Fig. 9, the percentages inhibition of Na-stimulated SO_4 uptake by DBDS were (mean ± SD, n = 4) 96 ± 9%, 90 ± 8%, 85 ± 1%, 80 ± 7% and 78 ± 11% at [DBDS] = 8, 16, 32, 64 and 100 μM, respectively. These results are very different from the data shown in Fig. 9, indicating that Na/SO_4 cotransport inhibited by low concentrations of DBDS is absent in BBMV. These results are consistent with the reported K_I of 350 μM for DIDS inhibition of Na-driven SO_4 uptake in rat BBMV [3].

It has been unclear whether the proximal tubule basolateral membrane contains Cl/SO_4 exchange, and whether pathways for Cl and SO_4 transport are distinct [15, 20, 23]. The $^{35}SO_4$ uptake results in Fig. 5 indicate that Cl gradients do *trans*-stimulate SO_4 uptake; however, the magnitude of the stimulation is less than that obtained for H and Na-gradient stimulation. To obtain independent evidence that Cl/SO_4 exchange is present, Cl transport was assayed using a Cl-sensitive fluorescent indicator introduced recently (*see* Materials and Methods) [16]. BLMV (voltage and pH clamped with K/valinomycin and nigericin) were subjected to a 50 mM inwardly directed Cl gradient in the absence of Na. Cl flux increased from 0.34 ± 0.02 nmole/sec/mg protein to 0.42 ± 0.02 nmol/sec/mg protein (mean ± SD, n = 4, $P < 0.002$) in the presence of 10 mM *trans*-SO_4, indicating that SO_4 gradients *trans*-stimulate Cl influx.

Discussion

We have used a site-specific fluorescent probe, DBDS, to characterize optically the renal basolateral membrane anion transporter. There are a number of applications of a probe which at some concentration binds specifically to membrane protein sites and undergoes a measureable change in fluorescence properties. (i) The probe can be used to identify optically tissues which contain specific binding sites. When viewed under a fluorescence microscope (excitation 360 nm, emission >400 nm), addition of 10 μM DBDS to suspended proximal tubules results in a marked signal over the tubule (and over red cells), but not in other structures. (ii) The probe can be used to examine the physical properties of the binding site. Studies of probe binding affinities, kinetics, and thermodynamics give information about protein conformation and subunit interactions; energy transfer experiments can be designed to determine distances between transporter binding sites. (iii) The mechanism of transport inhibition by the probe or by other inhibitory compounds can be examined from the effects of transported substrates and inhibitors on probe binding, and (iv) The probe can be used potentially to label the transporter for isolation and reconstitution studies.

DBDS has been used previously to study band 3 structure and function in human red blood cells. Based on equilibrium and kinetic studies of DBDS binding to red cell ghost membranes in the absence of transportable anions, it was concluded that DBDS binds initially to a low affinity site on one monomer of a band 3 dimer. The initial binding is followed by a protein conformational change which increases the affinity for the DBDS molecule already bound, and modifies the binding site on the second band 3 monomer to decrease its binding affinity for a second DBDS molecule [7, 28]. Based on the effects of Cl on DBDS binding, it was shown that Cl and DBDS possess distinct binding sites on band 3 which interact in a noncompetitive manner

[6]. DBDS binding has also been used recently to estimate the target size for the band 3 stilbene binding site by radiation inactivation [30].

The characteristics of the DBDS binding site on BLMV are notably different from those in the red cell membrane. In the absence of transportable anions, the DBDS-binding dissociation constant is ~3 μM on BLMV, whereas the high affinity K_d is 0.06 μM on red cell ghost membranes [28]. Interestingly, K_d for DBDS binding to ghost membranes is 3 μM before the conformational change occurs which "locks" DBDS into a high affinity state on the first monomer of the band 3 dimer, raising the possibility that the BLMV anion transporter lacks the ability to accommodate the DBDS molecule by a conformational alteration. The K_d for DBDS binding increases in the presence of transportable anions for both band 3 and for the BLMV anion transporter.

In BLMV, the apparent rate of DBDS binding decreases in the presence of transportable anions, whereas in ghost membranes, the rate increases. The findings in BLMV are compatable with competitive binding of DBDS and anions at a single binding site, whereas the results in ghost membranes require a noncompetitive interaction between transportable anions and DBDS. The independence of the apparent DBDS binding rate on [DBDS] in BLMV indicates that the rate-limiting binding reaction is a unimolecular step, or equivalently, a conformational change. The rates of the conformational change for BLMV isolated from rat and rabbit are approximately equal (5–6 sec^{-1}) and similar to that measured in ghost membranes (4 sec^{-1}). Thus, both similarities and notable differences exist in the characteristics of stilbene binding to anion transporters in the red cell and renal basolateral membranes.

The DBDS binding experiments define a class of stilbene binding sites on a basolateral membrane anion transport protein which has specificity for SO_4, HCO_3 and Cl. Based on measurements of the fluorescence of maximally bound DBDS on BLMV relative to that on red cell ghost membranes, it was estimated that ~20% of BLMV membrane protein is the DBDS-binding protein, and probably the anion transporter. The DBDS-binding experiments do not address directly the characteristics of the anion transporter and whether a heterogeneous population of anion transporters are present.

Several modes of anion transport were characterized on rabbit BLMV from $^{35}SO_4$ uptake and SPQ fluorescence measurements. There is an anion exchanger with broad specificity which exchangers SO_4 with SO_4, Cl, HCO_3, PO_4 and a number of organic anions. SO_4 transport is also driven by H gradients in the absence of CO_2 and by Na gradients. Under experimental conditions used, each mode of anion transport is electroneutral and inhibited by stilbenes, furosemide, probenecid and chlorothiazide, but not by amiloride and acetazolamide. Several properties of H and Na-gradient driven SO_4 uptake are different, including the anion *cis*-inhibition, SO_4 *cis*-inhibition and DBDS inhibition, suggesting that H and Na-gradient driven SO_4 uptake processes may be separate.

SO_4 transport mechanisms have been studied in brush border and basolateral membranes isolated from a number of renal and intestinal epithelia. In BBMV isolated from dog kidney, a SO_4 efflux pathway inhibited weakly by DIDS was identified using buffer containing Na [14]. Similarly, in BBMV isolated from rat kidney, Na driven SO_4 transport was characterized with a K_I of 350 μM for DIDS [3]. In contrast, the rabbit ileal BBMV has both Na and H driven SO_4 transport inhibited by stilbenes and furosemide [1, 19, 26]. In the flounder renal tubule BBMV, a neutral SO_4/anion exchanger has been found which is inhibited by stilbenes and probenecid, with half-maximal activation at 5 mM SO_4 [25].

In BLMV isolated from rat kidney, H, Na and Cl driven SO_4 transport have been identified, similar to our results obtained using BLMV isolated from rabbit kidney [3, 20]. K_I for DIDS inhibition of H driving SO_4 uptake was 2.4 μM with half-maximal activation at 5.4 μM SO_4. The substrate and inhibitor specificities for the rat BLMV anion transporter were similar to those reported in the present study. A similar DIDS-sensitive, H and anion driven SO_4 transporter was studied in BLMV isolated from rat jejunum [15]. In addition, a neutral, DIDS-sensitive, H driven SO_4 transporter has been identified in BLMV isolated from the Teleost renal tubule [24]. In the human red blood cell, band 3 is known to mediate SO_4/anion exchange with broad anion specificity, as well as H gradient driven SO_4 transport in the absence of HCO_3 [22].

It is not certain how many distinct renal BLMV anion transporters exist. The electrogenic Na/$3HCO_3$ cotransporter recently identified on basolateral membranes in rat and rabbit proximal tubule is probably distinct from the SO_4 transporter studied here [2, 11]. Unlike the SO_4 transporter, the Na/$3HCO_3$ cotransporter is electrogenic, requires HCO_3, and is inhibited only at high stilbene concentrations. A Na-independent, neutral Cl/HCO_3 exchanger was identified on BLMV isolated from rabbit kidney which was inhibited by DIDS, furosemide and probenecid [12]. Recently, we used a Cl-sensitive fluorescent indicator to measure the time course of intravesicular Cl in rabbit BLMV in response to ion gradients [5]. H gradient driven Cl transport in the presence and absence of HCO_3 was found to be neutral and inhibited by H_2DIDS. In addition a Cl flux *trans*-stimulated by Na was identified which required HCO_3 but not K; this transport

system probably represents Na/Cl/2HCO_3 coupled transport. There was no evidence to support the presence of a voltage-sensitive Cl conductance or a K/Cl cotransporter.

Therefore there probably exist at least three and possibly more distinct anion transport proteins in the rabbit proximal tubule basolateral membrane: neutral anion/anion exchange and Na/anion cotransport, and electrogenic Na/3HCO_3 cotransport. It is unclear whether the Na/Cl/2HCO_3 transport system represents a mode of the Na/anion cotransporter, or whether it is a different system. In general, the basolateral membrane neutral anion transporters have high affinity for stilbenes (<20 μM). The DBDS binding site(s) defined in the present studies, although described as a single saturable binding site, probably represent(s) a heterogeneous population of binding sites on distinct anion transport proteins with overlapping anion specificities. For this reason, quantitative comparisons of anion effects on DBDS and DBDS inhibition of anion transport are not possible. These comparisons were possible in the red cell system [7] because of the presence of a single protein (band 3) comprising ~50% of total membrane protein.

Recognizing these limitations in the analysis of data obtained in the basolateral membrane system, we can conclude: (i) DBDS binds to saturable stilbene binding site(s) on the basolateral membrane where it undergoes a fluorescence enhancement. There is little measureable DBDS binding on the brush border membrane. (ii) DBDS and anion binding, for a wide range of anions, is apparently competitive at an anion binding site. (iii) The rabbit proximal tubule basolateral membrane contains neutral, stilbene-inhibitable anion/SO_4 exchange and Na-driven SO_4 cotransport which are probably mediated by distinct proteins. In independent experiments, the basolateral membrane also contains neutral Cl/OH(HCO_3) countertransport and Na/Cl/2HCO_3 coupled transport. (iv) The basolateral membrane anion transport processes are inhibited by DBDS, likely at the stilbene binding site(s) observed in DBDS binding studies. Further definition of the molecular size and physical characteristics of basolateral membrane anion transport proteins will require labeling, isolation and reconstitution studies.

This work was supported by grants DK35124 and DK39354 from the National Institutes of Health, and an American Heart Association grant-in aid with partial support from the Long Beach Chapter and a grant from the National Cystic Fibrosis Foundation. Dr. Chen acknowledges the support of Drs. Hong-Sheng Lee, Shiann Pan and Tsu-Che Wang and was supported in part by the Department of Medicine, Taipei Medical College, Republic of China.

References

1. Ahearn, G.A., Murer, H. 1984. Functional roles of Na^+ and H^+ in SO_4^{2-} transport by rabbit ileal brush border membrane vesicles. *J. Membrane Biol.* **78:**177–186
2. Akiba, T., Alpern, R.J., Eveloff, J., Calamina, J., Warnock, D.G. 1986. Electrogenic sodium-bicarbonate cotransport in rabbit renal cortical basolateral membrane vesicles. *J. Clin. Invest.* **78:**1472–1478
3. Bastlein, C., Burckhardt, G. 1986. Sensitivity of rat renal luminal and contraluminal sulfate transport systems to DIDS. *Am. J. Physiol.* **250:***F*226–*F*234
4. Booth, A.G., Kenny, A.J. 1974. A rapid method for the preparation of microvilli from rabbit kidney. *Biochem. J.* **142:**575–581
5. Chen, P.-Y., Verkman, A.S. 1988. Sodium-dependent chloride transport in basolateral membrane vesicles isolated from rabbit proximal tubule. *Biochemistry (in press)*
6. Dix, J.A., Verkman, A.S., Solomon, A.K. 1986. Binding of chloride and a disulfonic stilbene transport inhibitor to red cell band 3. *J. Membrane Biol.* **82:**211–223
7. Dix, J.A., Verkman, A.S., Solomon, A.K., Cantley, L.C. 1979. Human erythrocyte anion exchange site characterized using a fluorescent probe. *Nature (London)* **282:**520–522
8. Dodge, J.T., Mitchell, C., Hanahan, D.J. 1963. The preparation and chemical characterization of hemoglobin-free ghosts of human erythrocytes. *Arch. Biochem. Biophys.* **100:**119–130
9. Forman, S.A., Verkman, A.S., Dix, J.A., Solomon, A.K. 1982. Interaction of phloretin with the anion transport protein of the red blood cell membranes. *Biochim. Biophys. Acta* **689:**531–538
10. Forman, S.A., Verkman, A.S., Dix, J.A., Solomon, A.K. 1985. Effect of halothane and *n*-alkanols on the red cell anion transport system. *Biochemistry* **24:**4859–4866
11. Grassl, S.M., Aronson, P.S. 1986. Na^+/HCO_3^- co-transport in basolateral membrane vesicles isolated from rabbit renal cortex. *J. Biol. Chem.* **261:**8778–8783
12. Grassl, S.M., Holohan, P.D., Ross, C.R. 1987. HCO_3 transport in basolateral membrane vesicles isolated from rat renal cortex. *J. Biol. Chem.* **262:**2682–2687
13. Grinstein, S., Turner, R.J., Silverman, M., Rothstein, A. 1980. Inorganic anion transport in kidney and intestinal brush border and basolateral membranes. *Am. J. Physiol.* **238:***F*452–*F*460
14. Guggino, S.E., Martin, G.J., Aronson, P.S. 1983. Specificity and modes of the anion exchanger in dog renal microvillus membranes. *Am. J. Physiol.* **244:**F612–F621
15. Hagenbuch, B., Stange, G., Murer, H. 1985. Transport of sulphate in rat jejunal and rat proximal tubular basolateral membrane vesicles. *Pfluegers Arch.* **405:**202–208
16. Illsley, N.P., Verkman, A.S. 1987. Membrane chloride transport measured using a chloride-sensitive fluorescent probe. *Biochemistry* **26:**1215–1219
17. Ives, H.E., Yee, V.J., Warnock, D.G. 1983. Asymmetric distribution of the Na/H antiporter in the renal proximal tubule epithelial cell. *J. Biol. Chem.* **258:**13513–13516
18. Kotaki, A., Naoi, M., Yagi, K. 1971. A diaminostilbene dye as a hydrophobic probe for proteins. *Biochim. Biophys. Acta* **229:**547–556
19. Langride-Smith, J.E., Field, M. 1981. Sulfate transport in rabbit ileum: Characterization of the serosal border anion exchange process. *J. Membrane Biol.* **63:**207–214
20. Low, I. Friedrich, T., Burckhardt, G. 1984. Properties of an

anion exchanger in rat renal basolateral membrane vesicles. *Am. J. Physiol.* **246:***F*334–*F*342

21. Lukacovic, M.F., Verkman, A.S., Dix, J.A., Solomon, A.K. 1984. Specific interaction of a water transport inhibitor with band 3 in red blood cell membranes. *Biochim. Biophys. Acta* **778:**253–259
22. Milanick, M.A., Gunn, R.B. 1984. Proton-sulfate cotransport: External proton activation of sulfate influx into human red blood cells. *Am. J. Physiol.* **247:***C*247–*C*259
23. Prichard, J.B., Renfro, J.L. 1983. Renal sulfate transport at the basolateral membrane is mediated by anion exchange. *Proc. Natl. Acad. Sci. USA* **80:**2603–2607
24. Renfro, J.L., Pritchard, J.B. 1982. H^+-dependent sulfate secretion in the marine teleost renal tubule. *Am. J. Physiol.* **243:***F*150–*F*159
25. Renfro, J.L., Pritchard, J.B. 1983. Sulfate transport by flounder renal tubule brush border: Presence of anion exchange. *Am. J. Physiol.* **244:***F*488–*F*496
26. Schron, C.M., Knickelbein, R.G., Aronson, P.S., Della Puca, J., Dobbins, J.W. 1985. pH gradient-stimulated sulfate transport by rabbit ileal brush border membrane vesicles: Evidence for SO_4-CH exchange. *Am. J. Physiol.* **249:***F*607–*F*613
27. Shimada, H., Burckhardt, G. 1986. Kinetic studies of sulfate transport in basolateral membrane vesicles from rat renal cortex. *Pfluegers Arch.* **407:***S*160–*S*167
28. Verkman, A.S., Dix, J.A., Solomon, A.K. 1983. Anion transport inhibitor binding to band 3 in red blood cell membranes. *J. Gen. Physiol.* **81:**421–449
29. Verkman, A.S., Ives, H.E. 1986. Water transport and fluidity in renal basolateral membranes. *Am. J. Physiol.* **250:***F*633–*F*643
30. Verkman, A.S., Skorecki, K.L., Jung, C.Y., Ausiello, D.A. 1986. Target molecular weights for the red cell band 3 stilbene and mercurial sites. *Am. J. Physiol.* **251:***C*541–*C*548

Received 26 May 1987